THE JOURNAL OF BIOLOGICAL CHEMISTRY VOL. 284, NO. 35, pp. 23312–23321, August 28, 2009

Acetylation of Histone H3 at the Nucleosome Dyad Alters DNA-Histone Binding*[S]

Received for publication, April 3, 2009, and in revised form, May 13, 2009 Published, JBC Papers in Press, June 11, 2009, DOI 10.1074/jbc.M109.003202

Mridula Manohar[‡], Alex M. Mooney[§], Justin A. North[§], Robin J. Nakkula[§], Jonathan W. Picking[‡§], Annick Edon[‡], Richard Fishel[¶], Michael G. Poirier[‡§1], and Jennifer J. Ottesen[‡2]

From the Departments of [‡]Biochemistry, [§]Physics, and [¶]Molecular Virology, Immunology, and Medical Genetics, Ohio State University, Columbus, Ohio 43210

Histone post-translational modifications are essential for regulating and facilitating biological processes such as RNA transcription and DNA repair. Fifteen modifications are located in the DNA-histone dyad interface and include the acetylation of H3-K115 (H3-K115Ac) and H3-K122 (H3-K122Ac), but the functional consequences of these modifications are unknown. We have prepared semisynthetic histone H3 acetylated at Lys-115 and/or Lys-122 by expressed protein ligation and incorporated them into single nucleosomes. Competitive reconstitution analysis demonstrated that the acetylation of H3-K115 and H3-K122 reduces the free energy of histone octamer binding. Restriction enzyme kinetic analysis suggests that these histone modifications do not alter DNA accessibility near the sites of modification. However, acetylation of H3-K122 increases the rate of thermal repositioning. Remarkably, Lys → Gln substitution mutations, which are used to mimic Lys acetylation, do not fully duplicate the effects of the H3-K115Ac or H3-K122Ac modifications. Our results are consistent with the conclusion that acetylation in the dyad interface reduces DNA-histone interaction(s), which may facilitate nucleosome repositioning and/or assembly/disassembly.

All eukaryotic genomes are organized into strings of nucleosomes, where 147 bp of DNA are tightly wrapped around a histone protein octamer (1). Many biological processes are dependent on DNA-protein interactions. However, access to DNA-binding sites is often restricted by the nucleosome structure. Alterations in nucleosome structure, dynamics, and positioning have been hypothesized to play a gatekeeper role in regulating biological processes such as DNA replication, repair, and transcription (2).

The post-translational modification (PTM)[3] of core histones (3) plays a central role in regulating the biological processing of eukaryotic genomes. Until recently, known histone PTMs were almost exclusively located on the unstructured histone tail regions, which extend from the structured core of the nucleosomes. PTMs in the histone tails can function to directly alter nucleosome (4–6) and/or chromatin structure and stability (7, 8) and function as protein-binding sites (9) in the "histone code" model (10).

During the past 5 years over 30 additional histone PTMs were identified within structured regions of the nucleosome (11–13). Many of these modifications are buried within the nucleosome core and thus are not readily accessible for protein binding. Fifteen of these histone PTMs are located in the DNA-histone interface, where the histone octamer contacts the phosphate backbone of the wrapped DNA (14). Studies have suggested that only mild structural perturbations occur in core-modified nucleosomes, which implies that modifications buried beneath the DNA are unlikely to provide a protein-binding site (15). This has led to two additional models for the function of nucleosome core PTMs.

Modifications such as Lys acetylation that reduce the positive charge of the histone octamer surface may reduce the binding affinity of histone-DNA interactions. In a "regulated nucleosome mobility model," these modifications would lead to increased mobility or "sliding" of nucleosomes between different positioning sites on DNA, often with the assistance of chromatin remodeling factors (14). DNA regulatory sites might be significantly more exposed as a result of such nucleosome movement (16). SIN (SWI/SNF-independent) histone mutations that are located in the nucleosome dyad appear to increase the rate of nucleosome repositioning following thermal heating (15, 17) and reduce DNA-histone interactions (18).

Alternatively, Widom and co-workers (19–21) have demonstrated that even a structured nucleosome undergoes fluctuations that render the nucleosome accessible via transient DNA unwrapping. In a "site accessibility model," side chain modifications that reduce the binding interactions between the histone octamer surface and DNA might modify the dynamics of the nucleosome structure and alter the proportion of DNA that is transiently unwrapped and accessible to regulatory factors.

* This work was supported, in whole or in part, by National Institutes of Health Grants CA067007 and GM062556 (to R. F.) and GM083055 (to M. P. and J. O.). This work was also supported by American Heart Association Predoctoral Fellowship 0815460D (to J. A. N.) and a Career Award in the Basic Biomedical Sciences from Burroughs Wellcome (to M. P.).

[S] The on-line version of this article (available at http://www.jbc.org) contains supplemental "Experimental Procedures," Figs. 1–4, and additional references.

[1] To whom correspondence may be addressed: 191 W. Woodruff, Columbus, OH 43210. Fax: 614-292-7557; E-mail: mpoirier@mps.ohio-state.edu.

[2] To whom correspondence may be addressed: 484 W. 12th St., Columbus, OH 43210. Fax: 614-292-6773; E-mail: ottesen.1@osu.edu.

[3] The abbreviations used are: PTM, post-translational modification; BZA, benzamidine; EPL, expressed protein ligation; H3-(1–109), residues 1–109 of histone H3, generated as a thioester; H3Pep, peptide with sequence CAIHAKRVTIMPKDIQLARRIRGERA; H3, full-length histone H3 protein; HO, histone octamer; mp2, modified high affinity 601 positioning sequence; MESNA, mercaptoethanesulfonic acid; RP-HPLC, reverse phase HPLC; MALDI-TOF-MS, matrix-assisted laser desorption ionization time-of-flight-mass spectrometry; ExoIII, exonuclease III.

Here we have tested aspects of these two models by examining Lys acetylation near the dyad symmetry axis of the nucleosome. The dyad represents a nexus of several interactions that include essential protein-protein contacts at the H3/H4 tetramer interface and histone-DNA contacts at the center of the positioned DNA sequence. The H3-K115 and H3-K122 residues are positioned between two histone DNA-binding motifs at the nucleosome dyad (Fig. 1). The side chain amines of these Lys residues are poised for electrostatic interactions with the DNA backbone. Because of inherent nucleosome symmetry, two copies of each amino acid exist in close spatial proximity; simultaneous modifications at these Lys residues would therefore create a patch of four histone modifications that could alter a large surface area in the assembled nucleosome (22).

Replacing H3-K115Q and H3-K122Q in yeast reduces transcriptional silencing at ribosomal DNA and telomeres (23). H3-K115R, which mimics constitutively unacetylated lysine, exhibits wild type silencing in both regions. However, H3-K122R exhibits wild type silencing in ribosomal DNA but reduced silencing in telomeres (23). Another study showed that H3-K115A and H3-K122A separately displayed reduced expression of the *PHO5* gene in budding yeast, whereas H3-K122A exhibited wild type expression (24). DNA repair also appears dependent on H3-K115 and/or H3-K122 acetylation. H3-K115Q increases sensitivity to hydroxyurea, whereas H3-K115R does not (23). Moreover, H3-K115A, H3-K122A, and H3-K122Q were all shown to be highly sensitive to Zeocin, a DNA double strand break mimetic (24). Whether the Lys → Gln mutations capture the entire features of Lys acetylation is a significant unknown.

To examine the precise role of Lys acetylation at the nucleosome dyad, we generated nucleosomes bearing acetylated Lys on histone H3-K115 and/or H3-K122 by expressed protein ligation (25–27). We found that the nucleosome position was not altered by H3-K115 and/or H3-K122 acetylation. However, competitive reconstitution analysis suggests that these H3 modifications reduced the free energy of binding between the histone octamer and a well defined nucleosome positioning DNA sequence. Restriction enzyme kinetic studies suggest that dynamic DNA site accessibility was not altered by the Lys modifications. However, the H3-K122Ac and H3-K115Ac/K122Ac nucleosomes demonstrated increased mobility in thermal repositioning studies. Remarkably, Lys → Gln substitution of these residues does not alter DNA-histone binding, suggesting that glutamine does not capture all the essential features of Lys-115 and Lys-122 acetylation. Our results are consistent with the conclusion that modifications of the nucleosome dyad alter nucleosome mobility and appear to support the regulated nucleosome mobility model.

EXPERIMENTAL PROCEDURES

Peptide Synthesis—Peptides were synthesized manually on *t*-butoxycarbonyl-Ala-PAM resin (Novabiochem) using standard *t*-butoxycarbonyl-N^{α} protection strategies and HBTU activation protocols. Selective Lys acetylation was accomplished by incorporation of Lys with orthogonal *N*-(9-fluorenyl)methoxycarbonyl side chain protection at the appropriate positions; prior to cleavage from the resin, the side chain amine was

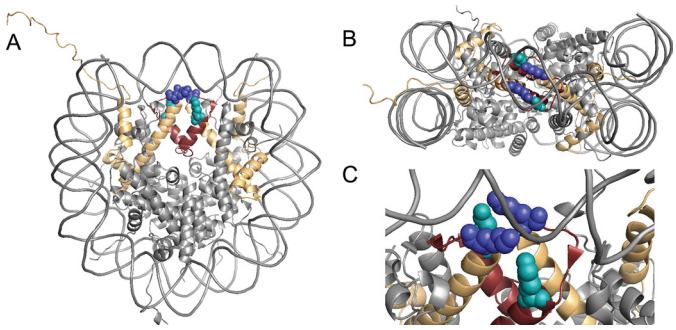

FIGURE 1. **H3-K115 and H3-K122 are buried below the DNA at the nucleosome dyad.** *A*, face view of the nucleosome (Protein Data Bank code 1AOI). H3 residues 1–109 are shown in *yellow*; residues 110–135 are shown in *red*. H3-K115 is shown as *blue spheres* and H3-K122 is shown as *teal spheres*. *B*, top view of the nucleosome; *C*, close-up view of the nucleosome dyad at 45° relative to *B* illustrates that H3-K115 and H3-K122 are positioned to interact with the DNA phosphate backbone.

revealed by treatment with 1:4 piperidine:*N*,*N*-dimethylformamide, and the side chain amine was acetylated with 1.5:1.5:7 acetic anhydride:diisopropylethylamine:*N*,*N*-dimethylformamide. Peptides were cleaved from the resin with standard HF cleavage procedures using p-cresol as a scavenger and purified by RP-HPLC on Vydac C-18 columns. Peptide purity was assessed as ≥95% using analytical RP-HPLC, and peptide identity was confirmed with MALDI-TOF-MS as follows: H3Pep-K115Ac, CAIHAK(Ac)RVTIMPKDIQLARRIRGERA (61 mg; *m*/*z* 3045.6 M + H, expected 3045.6 M + H); H3Pep-K122Ac, CAIHAKRVTIMPK(Ac)DIQLARRIRGERA (137 mg; *m*/*z* 3045.7 M + H, expected 3045.6 M + H); H3Pep-DualMod, CAIHAK(Ac)RVTIMPK(Ac)DIQLARRIRGERA (117 mg; *m*/*z* 3087.7 M + H, expected 3087.7 M + H).

Expression and Purification of Wild Type and Mutant Histones—Plasmids encoding histones H2A, H2B, H3, and H4 were the generous contributions of Dr. Karolin Luger (Colorado State University) and Dr. Jonathan Widom (Northwestern University). Mutations K115Q, K122Q, and K115Q/K122Q were introduced into histone H3 by site-directed mutagenesis (Stratagene). The expression and purification of wild type histones and mutant histones, H3-K115Q, H3-K122Q, and H3-K115Q/K122Q, were performed according to published protocols (28).

H3-(1–109) Thioester Production—Truncated histone H3 (residues 1–109) was cloned as a fusion protein with the GyrA intein and a chitin binding domain into the pTXB1 vector (New England Biolabs). The protein was expressed in *Escherichia coli* BL21 (DE3) cells and purified from inclusion bodies (see supplemental material), and the purified protein was refolded by dialysis into a high salt buffer. Thiolysis was initiated by addition of 100 mM MESNA and allowed to continue for 24 h at 4 °C (Fig. 2*B*). Buffer components were adjusted to generate ligation buffer (50 mM HEPES (pH 7.5), 6 M urea, 1 M NaCl, 1 mM EDTA, 50 mM MESNA), and the protein was concentrated to >1 mg/ml of the thioester and stored at −80 °C. Residual full-length H3-(1–109)-intein and cleaved intein remain in the sample through the ligation reaction; UV spectroscopy was used to determine total protein concentration, and thioester concentration was determined by characterization of cleavage yield by SDS-PAGE.

H3 Expressed Protein Ligation—Ten molar equivalents of the appropriate peptide were added to the concentrated protein thioester solution in ligation buffer (6 M urea, 1 M NaCl, 50 mM HEPES (pH 7.5), 1 mM EDTA, 20 mM tris(2-carboxyethyl)phosphine) and ligation proceeded overnight at room temperature with gentle agitation (Fig. 2*B*). The ligation mixture was dialyzed into water and lyophilized. The dry powder was resuspended in TrisU-100 (10 mM Tris (pH 9.0), 7 M urea, 1 mM EDTA, 5 mM EDTA, 5 mM β-mercaptoethanol, 100 mM NaCl) and purified by HPLC ion exchange chromatography (supplemental Fig. 1*A*) over a TSKgel SP-5PW column (TOSOH Bioscience). Full-length semisynthetic H3 and truncated H3-(1–109) could not be fully separated by this method; all fractions containing full-length H3 were combined, dialyzed extensively against water with 5 mM β-mercaptoethanol, and stored as the lyophilized powder at −80 °C. Protein yields were determined by UV spectroscopy, and proteins were isolated in up to a 7-mg yield of a 50:50 mixture of H3-K115Ac, K122Ac:H3-(1–109).

DNA Constructs—The mp2-192 and mp2-247 DNA molecules were prepared by PCR from the plasmid pMP2 (29). Each oligonucleotide (Sigma) was labeled with a Cy3 or Cy5 NHS ester (GE Healthcare) at an amino group attached to the 5′ end and then purified by RP-HPLC with a 218P^{TM} C18 (Grace/Vydac) column. The Cy5-labeled oligonucleotides used to amplify mp2-192 were as follows: Cy5-AGTGAATTCCGGTTGACGAGGTGCG and Cy5-GCTCGGTCCGACAGGATGTA. The Cy3- or Cy5-labeled oligonucleotides used to amplify mp2-247 were as follows: Cy3-TGTAAAACGACGGCCAGTGAATTCCGGTTG and Cy5-AAGCTTGCATGCAGATCTATGTCGGGCT. Following PCR amplification, each DNA molecule was purified by HPLC with a Gen-Pak Fax column (Waters). The unlabeled mp2-192 and mp2-247 DNA molecules were prepared by PCR with the same unlabeled oligonucleotides and then purified by RP-HPLC. 168-bp competitor DNA was prepared by PCR from pUC19 with oligonucleotides ACGTTGTTGCCATTGCTACAGGC and AACTTACTTCTGACAACGATCGGAGGAC and then purified by RP-HPLC.

Histone Octamer Refolding and Purification—The histone octamer refolding and purification procedure was modified from previously described methods (28). Briefly, each histone was unfolded for 1–3 h in unfolding buffer, 7 M guanidine, 20 mM Tris (pH 7.5), and 10 mM dithiothreitol, at a histone concentration of 2–20 mg/ml and then spun to remove aggregates. The absorption at 276 nm was measured for each unfolded histone to determine the concentration. The four core histones were combined at equal molar ratio with total histone concentration adjusted to 5 mg/ml in 200 μl. The octamer was refolded by double dialysis in refolding buffer: 2 M NaCl, 10 mM Tris-HCl (pH 7.5), 1 mM EDTA, and 5 mM β-mercaptoethanol. The recovered refolded octamer was centrifuged to remove large aggregates and then purified over a Superdex 200 (GE Healthcare) column to remove any H3/H4 tetramer (often containing truncated H3-(1–109)) or protein dimers. The purity of each octamer was confirmed by SDS-PAGE (supplemental Fig. 1*B*) and mass spectrometry (Fig. 2, *C* and *D*).

Nucleosome Reconstitutions—Nucleosomes for restriction enzyme analysis, thermal shifting, and exonuclease III mapping were reconstituted by salt double dialysis (30) with 0.5 μg of Cy3- and Cy5-labeled mp2-192 or mp2-247 DNA (Fig. 3*A*), 4.5 μg of competitor DNA, and 4 μg of purified HO that contained 0, 1, or 2 modifications or mutations. The DNA and HO were mixed in 50 μl of 0.5× TE (pH 8.0) with 2 M NaCl and 1 mM BZA. The sample was loaded into an engineered 50-μl dialysis chamber that was placed in a large dialysis tube with 80 ml of 0.5× TE (pH 8.0) with 2 M NaCl and 1 mM BZA. The large dialysis tube was extensively dialyzed against 0.5× TE with 1 mM BZA. The 50-μl sample was extracted from the dialysis button and purified by sucrose gradient centrifugation (Fig. 3*D*).

Competitive Reconstitutions—Competitive reconstitutions were modified from published protocols to measure the change in DNA-histone binding induced by K115Ac and/or K122Ac (30, 31) (see supplemental material). Reconstitutions were prepared in 2 M NaCl, 0.5× TE, 1 mM BZA with 1 ng/μl labeled MP2 DNA, 9 ng/μl unlabeled MP2 DNA, 40 ng/μl buffer DNA, and 8 ng/μl of HO (either unmodified, modified or mutated) in a volume of 40 μl. To minimize variation in DNA and HO concentrations, we first prepared a master mix that was combined with each HO stock, diluted to a concentration of 96 ng/μl in 2 M NaCl, 0.5× TE, and 1 mM BZA. Each HO sample was then split into thirds and dialyzed separately.

Each sample was dialyzed against the same reservoir containing 1.5 liters of 2 M NaCl, 0.5× TE, and 1 mM BZA. The concentration of salt in the dialysis reservoir was slowly reduced to 200 mM over 24 h; the samples were then dialyzed overnight against 0.5× TE and 1 mM BZA to reduce the final NaCl concentration to <1 mM NaCl. The reconstitution products were examined by PAGE, scanned with a Typhoon 8600 variable mode imager (GE Healthcare), and analyzed with ImageQuant (GE Healthcare).

Restriction Enzyme Kinetics Method for Site Accessibility—The restriction enzyme kinetics method (21) was used to determine the nucleosomal DNA accessibility, which is defined as the equilibrium constant for site exposure, $K_{eq} = k_{12}/k_{21}$, at the following five separate restriction enzyme sites: HindIII, HaeIII, Taq$^{\alpha}$I, HhaI, and PmlI (Fig. 5) (see supplemental material).

The reactions were initiated by mixing 50 μl of 2× restriction enzyme (New England Biolabs) and 50 μl of 2 nM nucleosomes. Taq$^{\alpha}$I digestion was carried out at 65, 47, and 37 °C, and all three temperatures resulted in the same relative equilibrium constant for site exposure; all other reactions were carried out at 37 °C. Time points at 1, 2, 4, 8, 16, 24, and 32 min were acquired by quenching 10 μl of the reaction with EDTA at a final concentration of 20 mM. Proteinase K (1 mg/ml final concentration) and SDS (0.02% final concentration) were added to each time point to remove the histone octamer from the DNA. Each time point was examined by native 5% PAGE (Fig. 5, *A* and *B*). The DNA was visualized with a Typhoon 8600 variable mode imager (GE Healthcare) and quantified by ImageQuant.

The digestions were fit to a single exponential to determine the initial digestion rate. An initial drop in undigested DNA between the 0 and 1-min time point is because of a small fraction of nucleosomes that dissociate during the rapid mixing.

We therefore neglect this initial time point as has been done in previous studies (21, 29).

Nucleosome Thermal Repositioning—Nucleosomes were thermally repositioned within the DNA substrate exactly as described previously (17). Sucrose gradient purified nucleosomes reconstituted with mp2-247 were diluted to a concentration of 200 nM in 50 mM Tris (pH 7.5). The nucleosomes were heated in a thermal cycler (Eppendorf) to 47, 50, 53, 59, or 65 °C. Nucleosome shifting occurred above 50 °C and dissociated above 59 °C before significant thermal shifting occurred. At 53 °C ~20% of the nucleosome shifted position although very little dissociated. Thermal shifting experiments were performed at 53 °C for 1, 2.5, 5, 10, 15, 20, 30, 45, and 60 min, and the reaction was stopped by transferring 10 μl of the heated nucleosomes to an ice water bath. Samples were analyzed by 5% PAGE in 0.2× TBE (Fig. 6, *A* and *B*). The gel was pre-run at 4 °C for 3 h before running the samples for 60 min at 30 V/cm at 4 °C with continuous recirculation of the running buffer. Following electrophoresis, the gels were imaged with a Typhoon 8600 variable mode imager (GE Healthcare) and quantified by ImageQuant.

Exonuclease III Mapping—The nucleosome positions within the mp2-247 DNA molecule were determined with ExoIII mapping. Reactions were carried out in an initial volume of 100 μl with 20 nM nucleosomes with 30 and 100 units of ExoIII (New England Biolabs) in Buffer 1 (New England Biolabs). At each time point, a 10-μl aliquot of the reaction was quenched with EDTA to a final concentration of 20 mM EDTA. A final concentration of 1 mg/ml of proteinase K and 0.02% of SDS was added to each time point to remove the histone octamer from the DNA, and samples were separated by 8% denaturing PAGE in 7 M urea and 1× TBE. The sequence markers were prepared with a SequiTherm Excel II DNA sequencing kit (Epicenter) using Cy3- or Cy5-labeled primers, an mp2-247 DNA template, and either dATP or dTTP. Results were imaged by a Typhoon 8600 variable mode imager (GE Healthcare), which detects Cy3 and Cy5 separately in the same gel (Fig. 7). The Cy3 and Cy5 ladders could be loaded in the same lanes to increase accuracy of the mapping gel readout. In parallel we carried out ExoIII digestions with naked DNA to confirm that none of the positions observed with nucleosomal DNA were because of exonuclease pause sites (data not shown).

RESULTS

Acetylated Lys-115 and/or Lys-122 Histone H3 Can Be Prepared by EPL and Refolded into the Histone Octamer—EPL is the chemoselective reaction between a polypeptide with an N-terminal Cys residue and a polypeptide with a C-terminal thioester moiety that generates a native polypeptide backbone with the Cys remaining at the ligation site (32, 33). The H3-K115 and H3-K122 acetylation sites are located at the nucleosome dyad and H3-H4 tetramer interface near the C terminus of histone H3 (Fig. 1). These sites are C-terminal to a natural Cys residue at position 110 that serves as an ideal ligation site for the introduction of synthetic peptides to generate a native H3 protein sequence after ligation (Fig. 2*A*). The H3-K115Ac and H3-K122Ac modifications were introduced via a synthetically accessible 26-residue peptide encompassing H3 residues 110–135. Peptides corresponding to each of the acetylation variants were synthesized and purified: H3Pep-K115Ac, H3Pep-K122Ac, and the dual-modified H3Pep-K115Ac/K122Ac.

The H3-(1–109)-intein fusion protein accumulated in inclusion bodies, as is typical for bacterially overexpressed histone proteins. The H3 fusion expression pattern is in contrast to a histone H2A-intein fusion protein, which has been reported to express as a soluble, well folded protein (27). Because a structured intein is required for the thiolysis reaction that generates the H3 thioester, we developed an intein refolding procedure in high salt conditions that maintains solubility of the H3 extein. Although we observed cleavage yields up to 90%, a typical intein thiolysis reaction proceeds to ~50% (Fig. 2*B*). We found that greater yields were obtained by simply denaturing and concentrating the cleavage mixture compared with thioester purification. Combining a 10-fold molar excess of the appropriate synthetic H3-(110–135) peptide with the concentrated cleavage mixture generated the full-length semisynthetic H3 histone (Fig. 2*B*).

The full-length H3 protein and H3-(1–109) may be co-purified using ion exchange chromatography (supplemental Fig. 1*A*). However, H3-(1–109) lacks a C-terminal α-helix that forms an essential protein-protein interface in the H3/H4 tetramer. When histone octamer is refolded from equimolar amounts of H2A, H2B, H3/H3-(1–109), and H4, only the full-length H3 is incorporated into the octamer, and the efficiency of refolding appears solely dependent on the full-length component of the H3 mixture. Histone octamer was refolded using the wild type unmodified H3, the three Gln mimic proteins, and three semisynthetic acetylated H3 variants. Both SDS-PAGE (supplemental Fig. 1*B*) and MALDI-MS analysis (Fig. 2, *C* and *D*) demonstrate that the H3-(1–109) fragment is completely eliminated from the histone octamer in each of the semisynthetic preparations and that the acetylation modifications survive purification. Interestingly, the fact that we efficiently refolded and purified histone octamer with either or both modifications suggests that H3-K115Ac and H3-K122Ac do not inhibit the formation of histone octamer.

Acetylation of H3-K115 and H3-K122 Does Not Inhibit Nucleosome Formation—We reconstituted nucleosomes with histone octamer containing H3-K115Ac and/or H3-K122Ac and DNA containing the high affinity nucleosome positioning sequence mp2, a variant of the 601 sequence (Fig. 3*A*) (29, 34). The reconstitutions were characterized by gel shift analysis on a native polyacrylamide gel and by sucrose gradient centrifugation (Fig. 3, *B–D*). Gel shift analysis is sensitive to changes in the overall structure of the nucleosome, such as changes in the position of the nucleosome on a DNA sequence (15, 17). We observed the electrophoretic mobility of the nucleosomes with H3-K115Ac and/or H3-K122Ac to be similar to unmodified nucleosomes. The rate of nucleosome sedimentation through a sucrose gradient depends on the mass and shape of the molecule. We find that the nucleosomes containing H3-K115Ac and/or H3-K122Ac sediment at the same rate as unmodified nucleosomes (Fig. 3*D*). These results suggest that the H3-K115Ac and/or H3-K122Ac modifications do not dramatically alter the nucleosome structure.

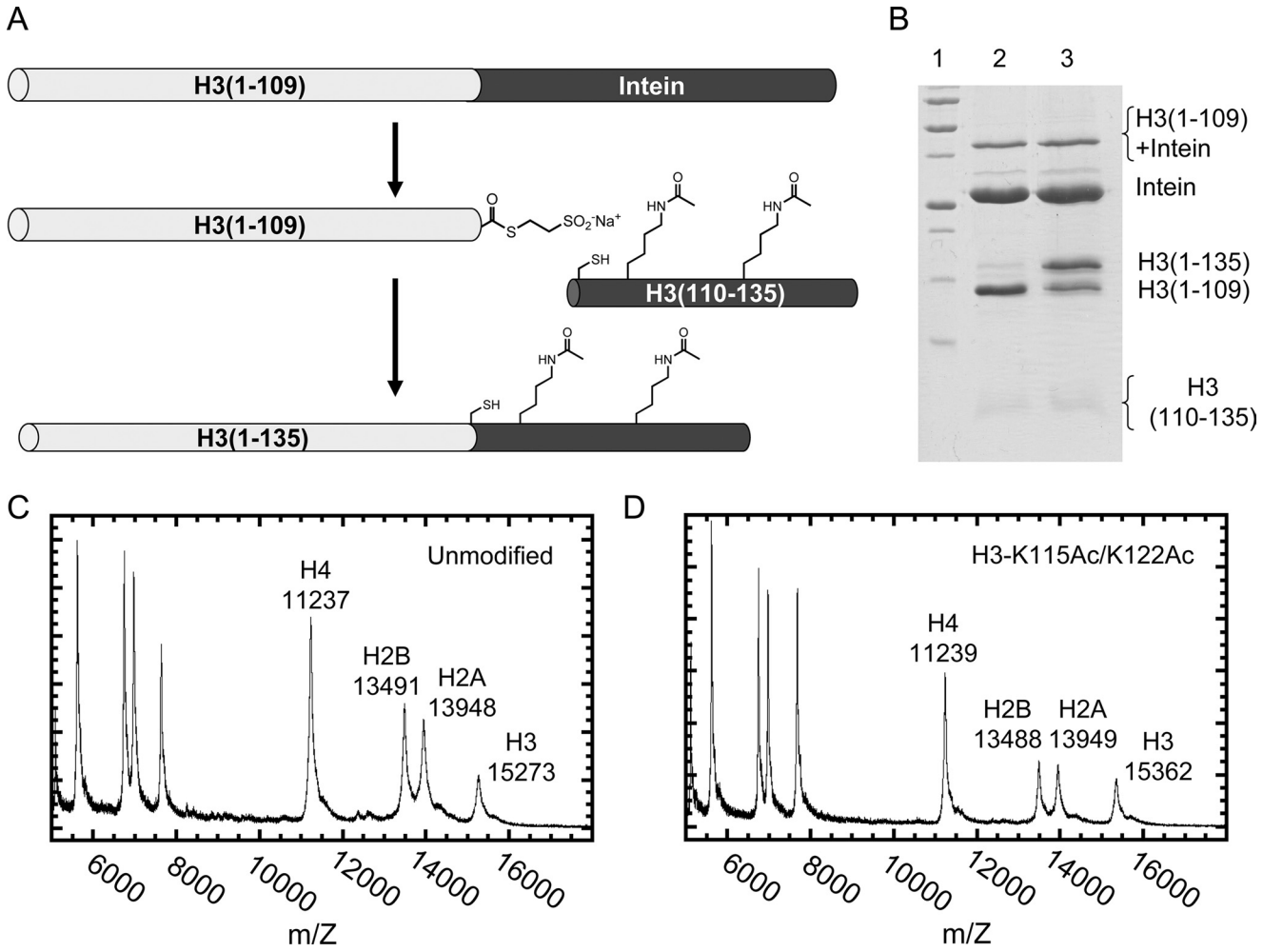

FIGURE 2. **Preparation of semi-synthetic histone octamers by expressed protein ligation.** *A,* EPL strategy for constructing histone H3 with Lys-115 and/or Lys-122 acetylated. *B,* SDS-PAGE analysis of a representative H3-K115Ac preparation. *Lane 1*, molecular weight standard. *Lane 2*, cleavage of the H3-(1–109)-intein fusion protein to generate H3-(1–109) thioester with 90% efficiency. *Lane 3*, H3Pep-K115Ac was added to the concentrated cleavage mixture, and overnight ligation yielded 60% full-length H3-K115Ac. *C*, MALDI-TOF mass spectrometry analysis of purified unmodified histone octamer. Note for H3, observed was *m/z* 15,273, and expected was 15,271. *D*, MALDI-TOF-MS of purified HO-K115Ac/K122Ac. Note for H3-K115Ac/K122Ac, observed was *m/z* 15,362, and expected was 15,355. H3-(1–109) would occur at *m/z* 12,285 if present.

Acetylation of Lys-115 and Lys-122 Reduces the Free Energy of the Histone Octamer Binding to a High Affinity Nucleosome Positioning Sequence—We performed nucleosome competitive reconstitutions (35) to examine the effect of H3-K115 and/or H3-K122 acetylation on the binding affinity of the histone octamer to DNA. Competitive reconstitutions were carried out as described previously (30) with the high affinity nucleosome positioning sequence mp2 (29) in the presence of an excess of low affinity competitor DNA. Under these conditions the free DNA and histone octamer establish a dynamic equilibrium with nucleosomes, and the equilibrium constant can be determined by gel shift analysis with native PAGE (30). We compared the binding equilibrium of specific histone octamer modifications to the binding equilibrium of the unmodified octamer to generate a $\Delta\Delta G$. Competitive reconstitutions with octamer containing H3-K115Ac, H3-K122Ac, or the doubly modified H3-K115Ac/K122Ac were performed at least three times, each in triplicate. In addition, for each semisynthetic construct, the reconstitution was repeated with histone octamer refolded from a separate EPL purification to confirm that the results were sample-independent.

An example of a competitive reconstitution analysis is shown in Fig. 4. The background-corrected K_{eq} was calculated from the ratio of gel-shifted nucleosomes to the free-DNA band (Fig. 4, *A* and *B*). We eliminated variations due to differences in each reconstitution by determining the equilibrium constant of the sample relative to the unmodified reference used in that reconstitution, $K_{eq\_sample}/K_{eq\_unmodified}$. The relative change in free energy of binding was calculated from $\Delta\Delta G = \Delta G_{sample} - \Delta G_{reference} = -k_B T(\ln(K_{eq\_sample})/(K_{eq\_reference}))$, where $k_B T =$ 0.55 kcal/mol for $T = 4$ °C. We find that H3-K115Ac induces a $\Delta\Delta G = 0.4 \pm 0.2$ kcal/mol, H3-K122Ac induces a $\Delta\Delta G$ of $0.2 \pm$ 0.2 kcal/mol, and the combination of both H3-K115Ac/K122Ac induces a $\Delta\Delta G$ of 0.6 ± 0.2 kcal/mol (Fig. 4*C*). These results demonstrate that the acetylation of H3-K115 and the simultaneous acetylation of H3-K115 and H3-K122 reduce the free energy of histone octamer binding by 0.4 and 0.6 kcal/mol, respectively. The acetylation of Lys-122 may also reduce the histone octamer affinity but appears within the uncertainty of our measurements.

Mutations That Mimic the Acetylation of Lys-115 and Lys-122 Do Not Reduce the Free Energy of the Histone Octamer

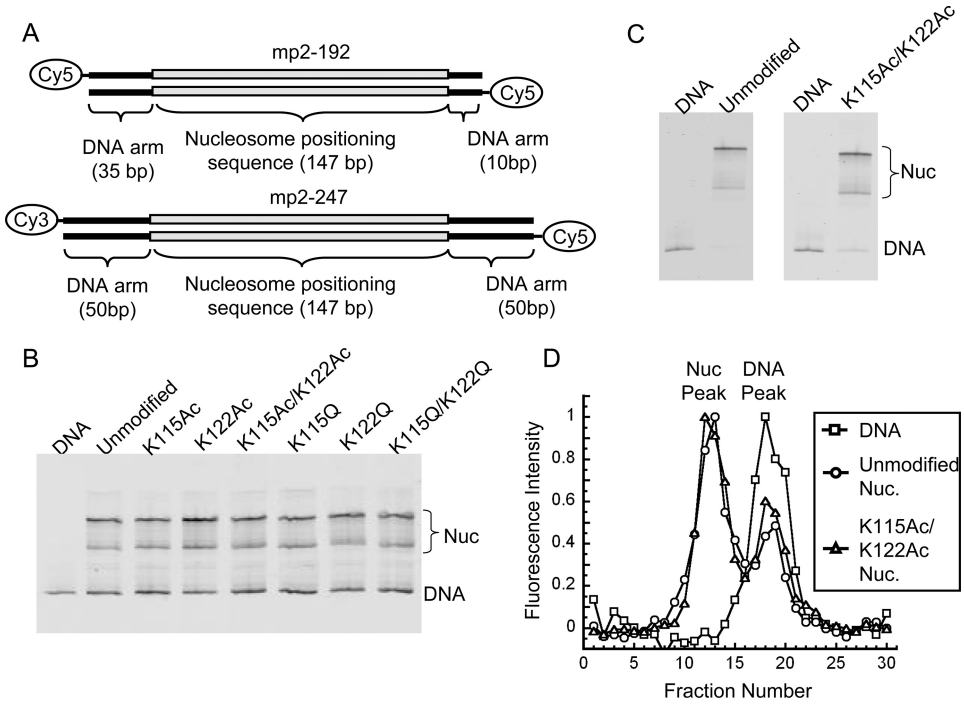

FIGURE 3. **Gel shift and sucrose gradient characterization of nucleosomes reconstituted with H3-K115 and/or Lys-122 acetylated or mutated to Gln.** *A*, two DNA constructs used throughout the experiments, which contain the altered 601 nucleosome positioning sequence mp2. mp2-192 is used in the competitive reconstitutions and the restriction enzyme experiments. mp2-247 is used in the thermal shift and exonuclease III experiments. *B*, PAGE analysis of seven different nucleosomes reconstituted with mp2-247 prior to purification; each lane is labeled with the HO used. The two bands represent two nucleosome (*Nuc*) positions. *C*, polyacrylamide gel shift characterization of nucleosomes reconstituted with mp2-247 DNA and purified by sucrose gradient fractionation to remove DNA. *D*, elution from the sucrose gradient was visualized by the Cy5 fluorescent label on the DNA. DNA in the absence of HO is included as a control.

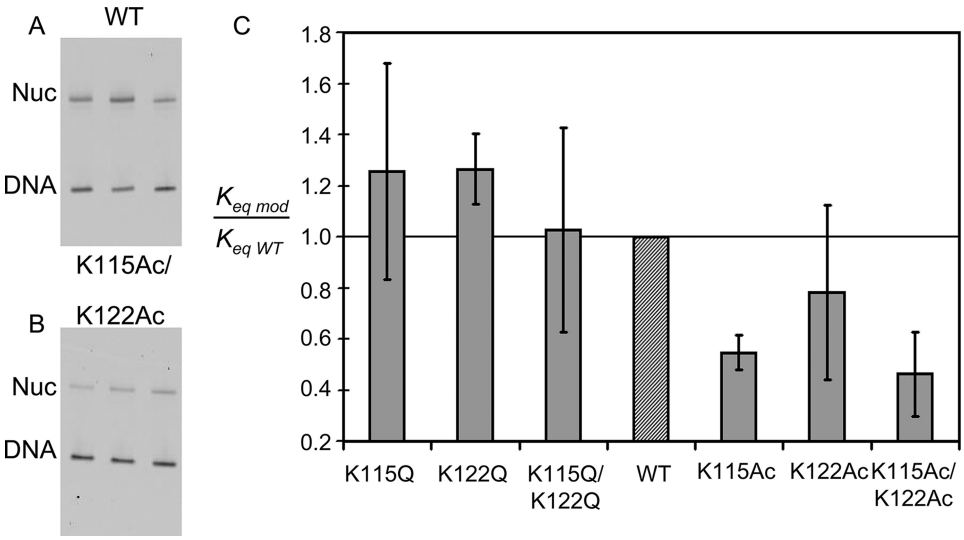

FIGURE 4. **Competitive reconstitution experiments determine how acetylation or glutamine substitution at the dyad alters DNA-histone binding affinity.** Native PAGE of a single reconstitution experiment using mp2-192 DNA for unmodified (*A*) and H3-K115Ac/K122Ac (*B*) nucleosomes (*Nuc*). For each experiment, an unmodified reconstitution was included as a reference. The ratio of the nucleosome band divided by the DNA band was used to determine a relative K_{eq}. Each experiment was repeated at least three times, each time in triplicate, such that each *bar* in *plot C* represents K_{eq} over at least nine data points. The *error bars* are the standard deviation. *WT*, wild type.

Binding to DNA—Lys → Gln substitution mutations are often used to simulate Lys acetylation *in vivo* (36). In fact, Lys → Gln substitutions in yeast studies were used to demonstrate the importance of H3-K115 and H3-K122 (23). To clarify the different influences of charge and steric bulk for locations buried at the histone-DNA interface, we examined histone octamer containing H3-K115Q and/or H3-K122Q by competitive reconstitution analysis. We found that the K_{eq} was not altered relative to the wild type unmodified histone octamer (Fig. 4*C*). These results demonstrate that the Lys → Gln substitution does not fully replicate the role of Lys acetylation. Moreover, it appears that Lys acetylation plays a role beyond simple electrostatic effects in the stability of the nucleosome.

Acetylation of H3-K115 and/or H3-K122 Does Not Alter DNA Unwrapping within the Nucleosome—To investigate the dynamics of nucleosome-DNA wrapping, we examined the kinetics of restriction enzyme digestions to determine site accessibility using unique sites that are located throughout the mp2 nucleosome localization sequence (supplemental Fig. 2, *A* and *B*). This method quantifies site accessibility as the equilibrium constant, K_{eq}, between the wrapped and unwrapped states of the nucleosome (supplemental Fig. 2, *C–E*), which is proportional to the forward rate of restriction enzyme digestion. The restriction enzyme kinetics studies were performed as described previously (21, 29), where K_{eq} for modified nucleosomes is determined relative to unmodified nucleosomes (Fig. 5, *A–C*).

We found that the forward rates of digestion for sites throughout the nucleosome were the same with and without H3-K115Ac and/or K122Ac, with a possible exception for the HindIII site (Fig. 5, *C* and *D*). The HhaI site is located directly above residues H3-K115 and H3-K122 at the midpoint of the wrapped DNA sequence. It might be anticipated that the accessibility of this site would be directly altered by the acetylation of these residues. However, the relative K_{eq} values for the HhaI site were 0.8 ± 0.1, 1.0 ± 0.4, and 1.2 ± 0.2 for H3-K115Ac, H3-K122Ac, and H3-K115/K122Ac, respectively. This result implies that there is no significant increase in the site exposure near the acetylated

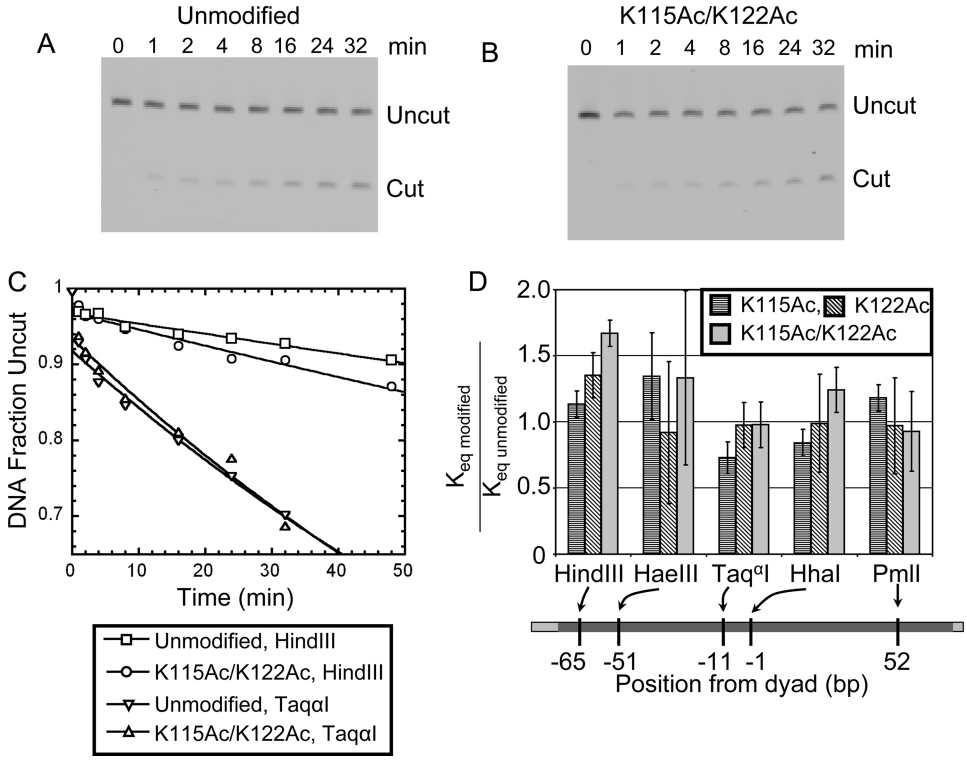

FIGURE 5. **Restriction enzyme kinetics determine the site accessibility of DNA throughout the nucleosome.** Representative PAGE analysis of Taq$^{\alpha}$I digestion with unmodified (*A*) or H3-K115Ac/K122Ac (*B*) nucleosomes reconstituted with mp2-192. Lanes are labeled with the time in minutes at which a time point was quenched. *C*, bands from each gel were quantified, and the course of the reaction was plotted as the fraction of DNA remaining uncut. Shown are HindIII digestions of unmodified (*squares*) and H3-K115Ac/K122Ac (*circles*) nucleosomes, and Taq$^{\alpha}$I digestions of unmodified (*inverted triangle*) and H3-K115Ac/K122Ac (*triangle*) nucleosomes. *D*, digestions were carried out at five different restriction sites, for unmodified and acetylated nucleosomes, in duplicate. The plot illustrates the average K_{eq} value for H3-K115Ac and/or H3-K122Ac nucleosomes relative to unmodified at each restriction site; *error bars* represent standard deviation. Each *bar* is placed at the relative position of the restriction site along the DNA sequence. Relative K_{eq} (H3-K115Ac) values are as follows: HindIII, 1.1 ± 0.1; HaeIII, 1.3 ± 0.3; Taq$^{\alpha}$I, 0.7 ± 0.1; HhaI, 0.8 ± 0.1; PmlI, 1.2 ± 0.1. Relative K_{eq} (H3-K122Ac) values are as follows: HindIII, 1.4 ± 0.2; HaeIII, 0.9 ± 0.5; Taq$^{\alpha}$I, 1.0 ± 0.2; HhaI, 1.0 ± 0.4; PmlI, 1.0 ± 0.4. Relative K_{eq} (H3-K115Ac/K122Ac) values are as follows: HindIII, 1.7 ± 0.1; HaeIII, 1.3 ± 0.7; Taq$^{\alpha}$I, 1.0 ± 0.2; HhaI, 1.2 ± 0.2; PmlI, 0.9 ± 0.3.

Lys residues. We conclude that site exposure is not altered in nucleosomes containing H3-K115Ac/K122Ac.

The HindIII site is particularly interesting and displays a relative K_{eq} of 1.1 ± 0.1, 1.4 ± 0.2, and 1.7 ± 0.1, for H3-K115Ac, H3-K122Ac, and H3-K115Ac/K122Ac, respectively. These results are consistent with an increased site exposure for H3-K122Ac and H3-K115Ac/K122Ac. The HindIII site is located about 4 nm from the acetylated Lys, making it unlikely that the modifications directly alter the DNA contacts stabilizing this region of the wrapped DNA. However, this site is 8 bp from the DNA entry-exit region of the nucleosome. One possible explanation is that the modifications might facilitate nucleosome repositioning that would place the HindIII site outside of the nucleosome.

Acetylation of H3-K122 Increases the Rate of Nucleosome Repositioning—The competitive reconstitutions demonstrated that the acetylation of H3-K115 and/or H3-K122 reduce the histone-DNA binding free energy, and restriction enzyme experiments suggested that they might also influence nucleosome repositioning. To investigate this possibility, we performed thermal repositioning studies as described previously (17). The thermal shifting experiments were carried out with purified nucleosomes reconstituted with the mp2 nucleosome positioning sequence and histone octamer containing either unmodified or H3-K115Ac and/or K122Ac (Fig. 6). The mp2 positioning sequence required higher temperatures to produce thermal shifting than previous studies (15, 17). The rate of repositioning was quantified by polyacrylamide gel shifts, because changes in nucleosome positions alter electrophoretic mobility (Fig. 6, *A* and *B*). We find that the top-shifted band decreases in intensity, although a new band appears just below it. The bottom-shifted band and the free DNA band remain relatively constant through the thermal shift experiment (Fig. 6, *C* and *D*).

To characterize the nucleosome positions before and after thermal shifting, we carried out ExoIII positional mapping (Fig. 7) (31). The DNA strands of the mp2 nucleosome localization sequence were independently 5′-labeled with Cy3 (top strand) or Cy5 (bottom strand) to allow visualization in a single denaturing gel. The location of nucleosome-independent ExoIII pause sites were determined by comparing the digestions to sequencing ladders that were prepared with a sequencing reaction that contained the same DNA molecule and either the Cy3- or Cy5-labeled DNA oligonucleotide.

Prior to heating, ExoIII stalled at 197 bp from the Cy5 5′-label (50 bp from the Cy3 end; see Fig. 7*A*) and 187, 197, and 201 bp from the Cy3 5′-label (60, 50, and 46 bp from the Cy5 end; see Fig. 7*C*). These positions imply that 147 bp are protected from ExoIII digestion and determine the dominant nucleosome position of the mp2 positioning sequence. The 187- and 201-bp stall sites that occur on the Cy3-labeled top strand do not have corresponding stall sites on the Cy5-labeled bottom strand. These data can be interpreted to suggest that the 201-bp stall position results from steric clash between the nucleosome and ExoIII. The 187-bp stall site is a likely result of partial nucleosome invasion by ExoIII. We can assign this dominant position to the upper band in the initial time point in the gel analysis of thermal shifting (Fig. 6, *A* and *B*).

We also observe a faint full-length band that survives initial ExoIII digestion for both the Cy5- and Cy3-labeled strands, as well as a Cy3 band that suggests ExoIII stalls 155 bp from the Cy3 end (Fig. 7, *A* and *C*). These additional ExoIII stall positions appear to indicate that a small fraction of the nucleosomes is positioned at the ends of the mp2 DNA. We can assign this position to the lower band in the thermal shifting gels (Fig. 6, *A*

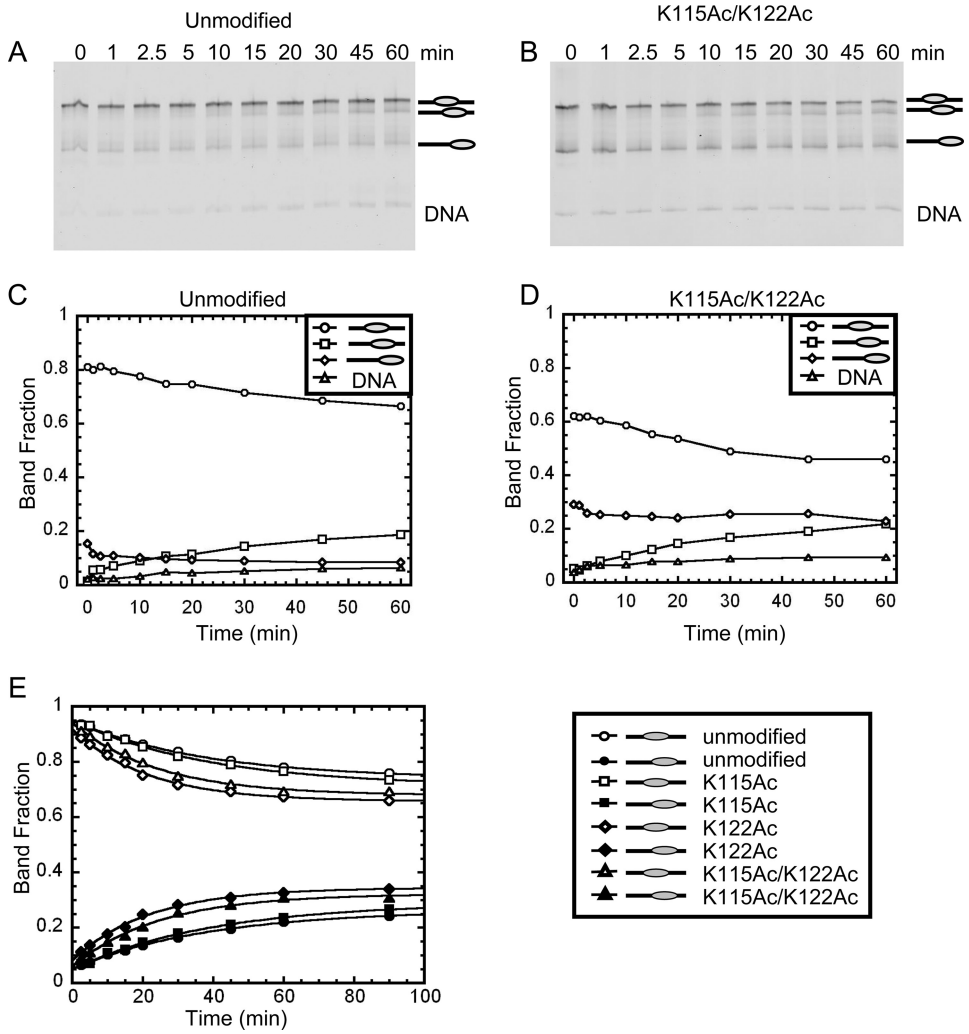

FIGURE 6. **Thermal shift experiments determine rates of heat-induced nucleosome repositioning.** Polyacrylamide gel shift analysis of thermal shifting at 53 °C for unmodified (*A*) and H3-K115Ac/H3-K122Ac (*B*) nucleosomes reconstituted with mp2-247 is shown. Lanes are labeled with the time (min) at which a point was acquired. The relative position of the nucleosome for each band is illustrated to the *right*. *C* and *D*, fraction of DNA in each band in *A* and *B* was quantified based on the Cy5 fluorescent label. *Circles* show the fraction in the dominant central nucleosome position. *Squares* show the fraction in the nucleosome position that appears with time, 20 bp toward the Cy5 end. *Diamonds* show the fraction of nucleosomes located at the end of the DNA. *Triangles* show the fraction of free DNA that remains. *E*, because free DNA and end-positioned nucleosomes remain constant, only the nucleosome fractions in the middle position (*open circle*, unmodified nucleosomes; *open square*, H3-K115Ac; *open diamond*, H3-K122Ac; *open triangle*, H3-K115Ac/K122Ac) and new shifted position (*filled circle*, unmodified nucleosomes; *filled square*, H3-K115Ac; *filled diamond*, H3-K122Ac; *filled triangle*, H3-K115Ac/K122Ac) were plotted. The curves were fit to a single exponential decay to determine that nucleosomes shift at 0.026 ± 0.002 min^{-1} when unmodified, at 0.025 ± 0.002 min^{-1} for H3-K115Ac, at 0.046 ± 0.003 min^{-1} for H3-K122Ac, and at 0.041 ± 0.004 min^{-1} for H3-K115Ac/K122Ac.

and *B*). In additional, both gel-shifted bands sediment on a sucrose gradient at the same rate (Fig. 3*D*), which suggests that they have similar mass. This combined with 147-bp protection strongly indicates that these bands contain canonical nucleosomes. We observe identical ExoIII mapping of unmodified nucleosomes before thermal shifting (supplemental Fig. 3, *A* and *C*).

Following thermal shifting, we found new ExoIII stall positions at 177 and 182 bp from the Cy5-labeled end and at 217 bp from the Cy3-labeled end (30 bp from the Cy5-labeled end and 70 bp from the Cy3-labeled end) (Fig. 7, *B* and *D*). These new pause sites suggest that the nucleosome is shifted 20 bp from the center of the mp2 sequence toward the Cy5 label and are consistent with protection of 147 bp of DNA, typical of a canonical nucleosome in the new position. This new position occurs for both unmodified histone octamer (supplemental Fig. 3, *B* and *D*) and histone octamer containing H3-K115Ac/K122Ac, and may be assigned to the middle gel band that appears with time during thermal shifting (Fig. 6, *A* and *B*). The mobility of each of the different nucleosome positions is consistent with previously reported thermal shift experiments (17).

We determined the rate of shifting to this new position by quantifying the bands containing each of the nucleosome positions and free DNA for unmodified nucleosomes and for nucleosomes containing H3-K115Ac and/or K122Ac (Fig. 6, *C* and *D*). The fraction of nucleosomes positioned within the mp2 sequence decreased with time, whereas the fraction of nucleosomes shifted by 20 bp toward the Cy5 end increased concurrently. Although there were variations in the fraction of nucleosomes initially positioned at the end of the mp2 DNA molecule in different nucleosome preparations, both the end-positioned fraction and the fraction of nucleosome-free DNA remained constant after the 1st min (Fig. 6, *C* and *D*). We conclude that the primary alteration in nucleosome position following thermal shift resulted in repositioning from the central location to 20 bp toward the Cy5 end.

We fit the fractions of positioned and shifted nucleosomes to a single exponential decay with an initial and final offset (Fig. 6*E*). We found unmodified nucleosomes shift with a rate of 0.026 ± 0.002 min^{-1}. Nucleosomes containing H3-K115Ac shifted with a rate of 0.025 ± 0.002 min^{-1}; nucleosomes containing H3-K122Ac shifted with a rate of 0.046 ± 0.003 min^{-1}, and nucleosomes containing H3-K115Ac/K122Ac shifted with a rate of 0.041 ± 0.004 min^{-1}. Thus, nucleosomes acetylated at H3-K122 with and without H3-K115Ac shift 1.6 ± 0.2 and 1.8 ± 0.2 times faster than unmodified nucleosomes. In contrast, nucleosomes acetylated only at H3-K115 shifted at nearly the same rate as unmodified nucleosomes. In addition, we observe that the fraction of repositioned nucleosomes is increased such that 20–25% more nucleosomes

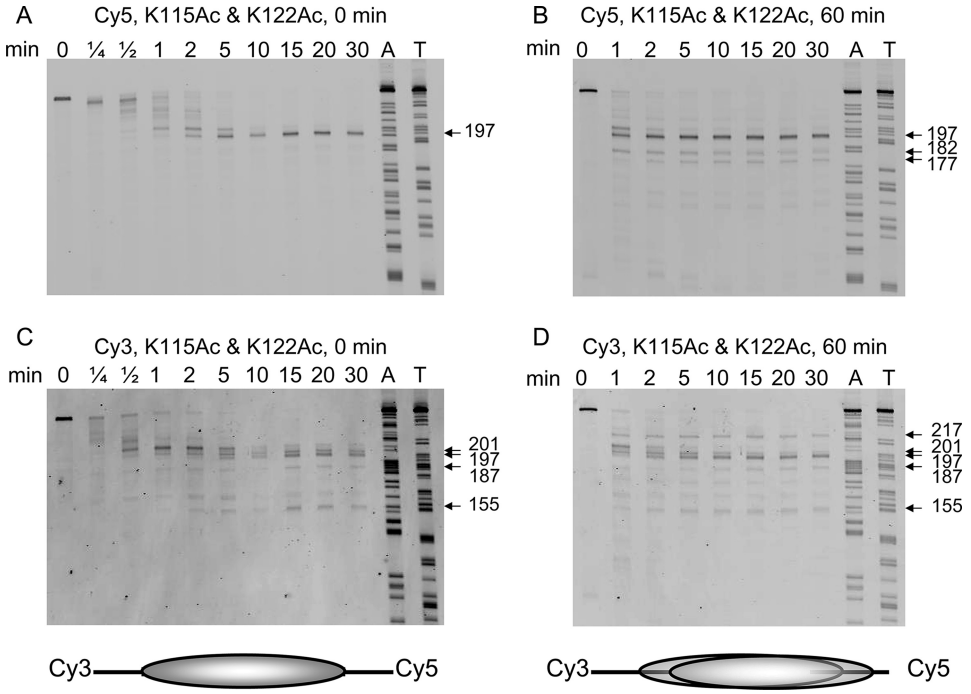

FIGURE 7. **Exonuclease III mapping to determine positions of nucleosomes.** Representative denaturing PAGE of exonuclease III mapping of H3-K115Ac/K122Ac nucleosomes reconstituted with mp2-247 before (*A*) and after (*B*) heating to 53 °C for 60 min and visualized using the Cy5 fluorescent label. Lanes are labeled with the time at which the exonuclease digestion was quenched. *C* and *D*, visualization of the gels from *A* and *B* using the Cy3 fluorescent label, which illustrates digestion from the other end of the DNA; a positioned nucleosome should protect 147 bp of DNA between the two digests. The new position that appears after heating is shifted 20 bp toward the Cy5-labeled end of the DNA relative to the mp2 positioning site. Similar results are also observed for unmodified nucleosomes (supplemental Fig. 3).

shift to the new position when they contain H3-K122Ac. Together these results are consistent with the conclusion that acetylation of H3-K122 increases nucleosome mobility.

DISCUSSION

Histone PTMs play key roles in essentially all biological processes that involve DNA-protein interactions. In this study, we have focused on two of the PTMs that are located in the DNA-histone interface of the nucleosome. Although genetic data demonstrate that these PTMs are important for RNA transcription and DNA repair, there is no information on how these modifications might alter nucleosome function(s).

Chemical tools to introduce distinct modifications into histone proteins (37) and the use of EPL to introduce histone modifications into unstructured histone tails (8, 27, 38) have proven to be an essential part of the study of chromatin structure. Here we report the first use of EPL to introduce modified residues into a folded histone domain in the nucleosome core. Because our approach generates the native protein sequence of histone H3, it has enabled us to precisely characterize the effects of buried modifications at the histone-DNA interface.

We find that histone octamers acetylated at H3-K115 and H3-K122 reduced the binding free energy to a DNA positioning sequence by 0.6 kcal/mol. Remarkably, histone octamers containing H3-K115Ac alone appear to account for the majority of the reduced binding free energy (0.4 kcal/mol). The $\Delta\Delta G$ of 0.6 kcal/mol is similar to the difference in free energy between genomic DNA and the natural 5 S nucleosome positioning sequence (30). In fact, the typical variation in binding free energy for genomic positioning sequences is ~0.5–1 kcal/mol (39). This implies that the $\Delta\Delta G$ values induced by these modifications are on the same scale as the typical variation in DNA-histone binding affinity caused by the DNA sequence *in vivo*. Taken as a whole, these observations suggest that the reduced affinity of nucleosomes containing H3-K115Ac and/or H3-K122Ac may directly influence the positioning of nucleosomes within the genome (39, 40).

Not only could the reduction in DNA-histone binding influence where nucleosomes are positioned, it may also influence DNA unwrapping from the histone octamer and/or nucleosome repositioning (41). Our restriction enzyme positioning studies demonstrate that the acetylation of H3-K115 and/or H3-K122 does not alter the probability of DNA site exposure to restriction enzymes. We note a modest increase in site accessibility with the double acetylated histone octamer near the DNA entry-exit region. It is formally possible that the dyad modifications directly influence DNA unwrapping near the DNA entry-exit region. We view this as unlikely because H3-K115 and H3-K122 are over 4 nm from the DNA entry-exit region of the nucleosome. Dramatic changes in the nucleosome structure would be required for the acetylation of these residues to directly reduce DNA wrapping and accessibility at the entry-exit region. Moreover, DNA site accessibility was not altered at sites between the dyad and the DNA entry-exit region, which would indicate propagation of unwrapping along the double helix. Instead, we consider the possibility that small changes in the nucleosome position could transiently expose sites near the DNA entry-exit region. Such an hypothesis would appear consistent with the modest increases in entry-exit site exposure of the double-acetylated histone octamer to a position that increases the exposure of the HindIII site while leaving the PmlI site near the other end of the nucleosome unchanged.

We found that the rates of thermal repositioning of histone octamers containing H3-K122Ac as well as H3-K122Ac and H3-K115Ac were modestly increased. Although 2-fold effects can be significant in gene expression, as is the case with dosage compensation and haploinsufficiency diseases, it seems more likely that these modifications do not singularly reposition nucleosomes *in vivo*. We regard it more likely that these modifications facilitate nucleosome repositioning in the presence of associated chromatin remodeling factors (16, 42).

Nucleosome assembly occurs in a stepwise fashion where the deposition of H3-H4 is followed by the deposition of H2A-H2B

(43). Nucleosome disassembly occurs in the reverse order (43). DNA-histone interactions in the dyad region of the nucleosome are likely to play an important role during the assembly/disassembly process. In general, histone modifications could be introduced prior to nucleosome formation to alter the rate of nucleosome assembly, or within chromatin to alter the rate of nucleosome disassembly. Dynamic modifications of H3-K115 and/or H3-K122 that are located within the histone-DNA dyad interface might serve as potential regulators of the assembly/disassembly process. The histone chaperone Asf1 is known to assemble and disassemble nucleosomes by loading and unloading H3-H4 dimers (44, 45). In this regard it is worth noting that the H3-K115 and H3-K122 residues are located near the Asf1-histone interface (24).

Lys acetylation is often mimicked by substituting Lys → Gln *in vivo*. Our comparison of acetylated lysine with the Lys → Gln substitution in competitive reconstitution studies found significant differences between the modification and the mimic. Our results appear to suggest that the Lys → Gln substitution mimics the change in charge but is a very poor mimic of the steric effects of acetylation. Previous studies have compared the effect of Gln and acetylated Lys located in the unstructured tail domains of histone proteins in higher order chromatin structure. In this context, Gln proved an effective mimic of the acetylated lysine (46). However, in the structured core domains of histones, Lys residues are restricted by contacts with the DNA backbone and within the histone octamer, and steric effects could play a more significant role in influencing the structure and stability of the nucleosome.

Acknowledgments—We thank K. Musier-Forsyth for access to a Typhoon Trio gel scanner and a fluorescence plate reader. We thank Joshua Wagner for preparing some of the H3-(1-109) protein used in this study. We thank Thomas Haver for help with the competitive reconstitution experiments and Kelsey Schafer for help with the thermal shifting experiments.

REFERENCES

1. Kornberg, R. D., and Thomas, J. O. (1974) *Science* **184,** 865–868
2. Fischle, W., Wang, Y., and Allis, C. D. (2003) *Curr. Opin. Cell Biol.* **15,** 172–183
3. Wang, G. G., Allis, C. D., and Chi, P. (2007) *Trends Mol. Med.* **13,** 363–372
4. Anderson, J. D., Lowary, P. T., and Widom, J. (2001) *J. Mol. Biol.* **307,** 977–985
5. Ura, K., Kurumizaka, H., Dimitrov, S., Almouzni, G., and Wolffe, A. P. (1997) *EMBO J.* **16,** 2096–2107
6. Widlund, H. R., Vitolo, J. M., Thiriet, C., and Hayes, J. J. (2000) *Biochemistry* **39,** 3835–3841
7. Kouzarides, T. (2007) *Cell* **128,** 693–705
8. Shogren-Knaak, M., Ishii, H., Sun, J. M., Pazin, M. J., Davie, J. R., and Peterson, C. L. (2006) *Science* **311,** 844–847
9. Taverna, S. D., Li, H., Ruthenburg, A. J., Allis, C. D., and Patel, D. J. (2007) *Nat. Struct. Mol. Biol.* **14,** 1025–1040
10. Strahl, B. D., and Allis, C. D. (2000) *Nature* **403,** 41–45
11. Zhang, K., Tang, H., Huang, L., Blankenship, J. W., Jones, P. R., Xiang, F., Yau, P. M., and Burlingame, A. L. (2002) *Anal. Biochem.* **306,** 259–269
12. Zhang, L., Eugeni, E. E., Parthun, M. R., and Freitas, M. A. (2003) *Chromosoma* **112,** 77–86
13. Cocklin, R. R., and Wang, M. (2003) *J. Protein Chem.* **22,** 327–334
14. Cosgrove, M. S., Boeke, J. D., and Wolberger, C. (2004) *Nat. Struct. Mol. Biol.* **11,** 1037–1043
15. Muthurajan, U. M., Bao, Y., Forsberg, L. J., Edayathumangalam, R. S., Dyer, P. N., White, C. L., and Luger, K. (2004) *EMBO J.* **23,** 260–271
16. Becker, P. B., and Hörz, W. (2002) *Annu. Rev. Biochem.* **71,** 247–273
17. Flaus, A., Rencurel, C., Ferreira, H., Wiechens, N., and Owen-Hughes, T. (2004) *EMBO J.* **23,** 343–353
18. Kurumizaka, H., and Wolffe, A. P. (1997) *Mol. Cell. Biol.* **17,** 6953–6969
19. Anderson, J. D., and Widom, J. (2000) *J. Mol. Biol.* **296,** 979–987
20. Li, G., and Widom, J. (2004) *Nat. Struct. Mol. Biol.* **11,** 763–769
21. Polach, K. J., and Widom, J. (1995) *J. Mol. Biol.* **254,** 130–149
22. Luger, K., Mäder, A. W., Richmond, R. K., Sargent, D. F., and Richmond, T. J. (1997) *Nature* **389,** 251–260
23. Hyland, E. M., Cosgrove, M. S., Molina, H., Wang, D., Pandey, A., Cottee, R. J., and Boeke, J. D. (2005) *Mol. Cell. Biol.* **25,** 10060–10070
24. English, C. M., Adkins, M. W., Carson, J. J., Churchill, M. E., and Tyler, J. K. (2006) *Cell* **127,** 495–508
25. He, S., Bauman, D., Davis, J. S., Loyola, A., Nishioka, K., Gronlund, J. L., Reinberg, D., Meng, F., Kelleher, N., and McCafferty, D. G. (2003) *Proc. Natl. Acad. Sci. U.S.A.* **100,** 12033–12038
26. Shogren-Knaak, M. A., and Peterson, C. L. (2004) *Methods Enzymol.* **375,** 62–76
27. McGinty, R. K., Kim, J., Chatterjee, C., Roeder, R. G., and Muir, T. W. (2008) *Nature* **453,** 812–816
28. Luger, K., Rechsteiner, T. J., and Richmond, T. J. (1999) *Methods Mol. Biol.* **119,** 1–16
29. Poirier, M. G., Bussiek, M., Langowski, J., and Widom, J. (2008) *J. Mol. Biol.* **379,** 772–786
30. Thåström, A., Lowary, P. T., and Widom, J. (2004) *Methods* **33,** 33–44
31. Thåström, A., Bingham, L. M., and Widom, J. (2004) *J. Mol. Biol.* **338,** 695–709
32. Ottesen, J. J., Bar-Dagan, M., Giovani, B., and Muir, T. W. (2008) *Biopolymers* **90,** 406–414
33. Muir, T. W. (2003) *Annu. Rev. Biochem.* **72,** 249–289
34. Lowary, P. T., and Widom, J. (1998) *J. Mol. Biol.* **276,** 19–42
35. Shrader, T. E., and Crothers, D. M. (1989) *Proc. Natl. Acad. Sci. U.S.A.* **86,** 7418–7422
36. Li, M., Luo, J., Brooks, C. L., and Gu, W. (2002) *J. Biol. Chem.* **277,** 50607–50611
37. Simon, M. D., Chu, F., Racki, L. R., de la Cruz, C. C., Burlingame, A. L., Panning, B., Narlikar, G. J., and Shokat, K. M. (2007) *Cell* **128,** 1003–1012
38. Ferreira, H., Flaus, A., and Owen-Hughes, T. (2007) *J. Mol. Biol.* **374,** 563–579
39. Segal, E., Fondufe-Mittendorf, Y., Chen, L., Thåström, A., Field, Y., Moore, I. K., Wang, J. P., and Widom, J. (2006) *Nature* **442,** 772–778
40. Yuan, G. C., Liu, Y. J., Dion, M. F., Slack, M. D., Wu, L. F., Altschuler, S. J., and Rando, O. J. (2005) *Science* **309,** 626–630
41. Mersfelder, E. L., and Parthun, M. R. (2006) *Nucleic Acids Res.* **34,** 2653–2662
42. Maier, V. K., Chioda, M., and Becker, P. B. (2008) *Biol. Chem.* **389,** 345–352
43. Park, Y. J., and Luger, K. (2008) *Curr. Opin. Struct. Biol.* **18,** 282–289
44. Adkins, M. W., Howar, S. R., and Tyler, J. K. (2004) *Mol. Cell* **14,** 657–666
45. Schwabish, M. A., and Struhl, K. (2006) *Mol. Cell* **22,** 415–422
46. Wang, X., and Hayes, J. J. (2008) *Mol. Cell. Biol.* **28,** 227–236